Accurate Detection of Arbitrary Photon Statistics

Josef Hloušek, Michal Dudka, Ivo Straka, and Miroslav Ježek*
Department of Optics, Palacký University, 17. listopadu 12, 77146 Olomouc, Czechia

(Received 16 December 2018; published 11 October 2019)

We report a measurement workflow free of systematic errors consisting of a reconfigurable photon-number-resolving detector, custom electronic circuitry, and faithful data-processing algorithm. We achieve an unprecedented accurate measurement of various photon-number distributions going beyond the number of detection channels with an average fidelity of 0.998, where the error is primarily caused by the sources themselves. Mean numbers of photons cover values up to 20 and faithful autocorrelation measurements range from $g^{(2)} = 6 \times 10^{-3}$ to 2. We successfully detect chaotic, classical, nonclassical, non-Gaussian, and negative-Wigner-function light. Our results open new paths for optical technologies by providing full access to the photon-number information without the necessity of detector tomography.

DOI: 10.1103/PhysRevLett.123.153604

The probability distribution of the number of photons in an optical mode carries a great deal of information about physical processes that generate or transform the optical signal. Along with modal structure and coherence, the statistics provides a full description of light. Precise characterization of photon statistics is a crucial requirement for many applications in the field of photonic quantum technology [1], such as quantum metrology [2,3], nonclassical light preparation [4,5], quantum secure communication [6], and photonic quantum simulations [7,8]. Measurement of statistical properties and nonclassical features of light also represents enabling technology for many emerging biomedical imaging and particle-tracking techniques [9–11]. Statistical correlations are routinely applied to quantify the nonclassicality of light [12,13]. Obtaining photon statistics requires repeated measurements using a photon-number-resolving detector (PNRD). The important parameters of PNRDs are dynamic range, speed, and accuracy.

The main result of our Letter is a photon-statistics retrieval method based on expectation-maximization entropy and implemented in a PNRD design that is virtually free of systematic errors. Our results show unprecedented accuracy across dozens of tested optical signals, ranging from a highly sub-Poissonian single-photon state to super-Poissonian thermal light with non-negligible multiphoton content up to $n = 30$. The accuracy is achieved despite leaving all systematic errors uncorrected and operating with raw data. The proposed method also provides faithful $g^{(2)}$ values [14] for states, where the commonly used Hanbury Brown–Twiss measurement would fail due to high multiphoton content [15].

We demonstrate the accuracy of the reported PNRD by performing photon-statistics measurements for many different states of light, from which 25 states are shown in Fig. 1, covering various mean photon numbers and $g^{(2)}$ values. Furthermore, the reconfigurability of the presented PNRD also allows for direct measurement of correlation functions and nonclassicality witnesses [5,16].

Contemporary PNRD technologies all rely on multiplexing with the exception of transition-edge detectors [4,17] that require temperatures below 100 mK, offer rates of 10–100 kHz, and suffer from range-versus-crosstalk compromise. Photon-number resolution using a single

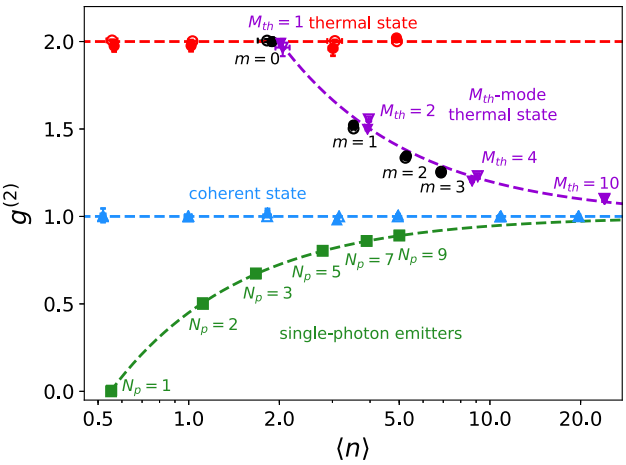

FIG. 1. The autocorrelation $g^{(2)}$ evaluated from the measured photon statistics (solid marker) and the corresponding ideal statistics (empty marker) of various optical signals with mean photon number $\langle n \rangle$ [14]. Shown are the coherent states with $g^{(2)} = 1$ (blue triangle up), thermal states (also termed chaotic light) with $g^{(2)} = 2$ (red circle), M_{th}-mode thermal states with $M_{\mathrm{th}} = 1, 2, 4, 10$ (violet triangle down), and m-photon-subtracted thermal states for $m = 0$, 1, 2, 3 (black circle). The cases of $M_{\mathrm{th}} = 1$ and $m = 0$ coincide with the thermal state. Furthermore, the emission from a cluster of N_p single-photon emitters is shown for $N_p = 1,\ldots,9$ with $g^{(2)} = 1 - 1/N_p$.

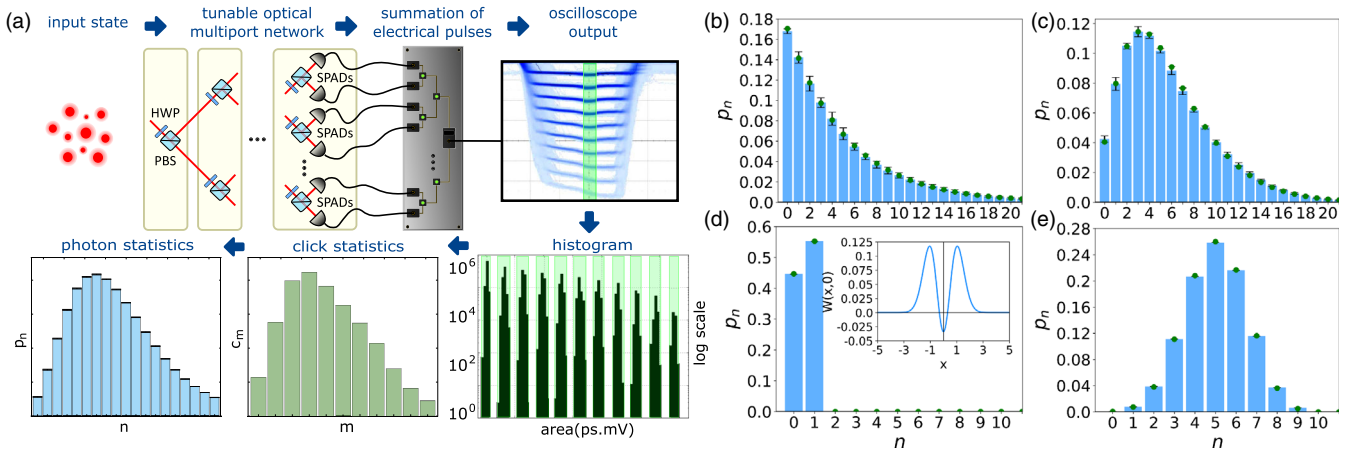

FIG. 2. (a) Experimental setup of the PNRD based on a discrete optical network with full reconfigurability and continuous tunability of splitting ratios, pulse-height spectrum of the analog output of the detector, and scheme of photon-statistics retrieval. Measured (blue bars) and the corresponding theoretical photon statistics (green dots) for (b) thermal state with $\langle n \rangle = 4.93(4)$, (c) two-photon-subtracted thermal state, (d) single-photon, and (e) heralded nine-photon state that emulates emission from a cluster of single-photon emitters. (Inset) Wigner function evaluated from the measured statistics. Note that the data agree with theory even beyond the number of channels of the PNRD (ten).

superconducting nanowire single-photon detector is also possible, but suffers from significant cross talk [18].

The multiplexing approach is based on dividing an input optical signal into multiple on-off detectors [19,20]. Many schemes of temporal and spatial multiplexing have been reported using bulk on-off detectors [21–25], integrated on-off pixels [26–31], or even a few photon-number-resolving detectors [4,32]. Though being economical in respect to the number of on-off detectors employed, the temporal multiplexed scheme trades off a decrease of the detector speed for an increase in a number of the detection channels. Decreasing the losses and the balancing of temporal multiplexors require a great deal of optimization [33] or even active signal switching [25]. On the other hand, multiple-pixel PNRDs typically suffer from strong cross talk effects, which demands an extensive characterization of the detector [34] and advanced numerical postprocessing to correct for the imperfections [28,30]. Also, the multipixel detectors offer very limited reconfigurability and complicate channel balancing. Recent on-chip integration of independent on-off cryogenic detectors represents a promising direction [29,31,35], which has yet to be tested for various classical and, particularly, nonclassical sources.

The reported photon-number-resolving detector is based on spatial multiplexing of the input photonic signal by a reconfigurable optical network as depicted in Fig. 2(a). The multiport network consists of cascaded tunable beam splitters composed of a half-wave plate (HWP) and a polarizing beam splitter (PBS), which allow for accurate balancing of the output ports or, if needed, changing their number so there is no need to physically add or remove detectors. The whole network works as a one-to-M splitter balanced with the absolute error below 0.3%. To measure the multiplexed signal, we use single-photon avalanche photodiodes (SPADs) with efficiency close to 70%, 250 ps timing jitter, and 25 ns recovery time. The electronic outputs of the SPADs are summed by a custom coincidence logic while keeping the individual channels synchronized. Alternatively, the output can be visualized using an oscilloscope, see Fig. 2(a). Each of the resulting $M+1$ distinct voltage levels corresponds to the particular number of m-fold coincidences. Repeated measurements give rise to click statistics. Full technical details are given in the Supplemental Material [36], including a discussion of processing electronic signals from single-photon detectors.

It is important to stress here that the PNRD operates in real time and yields a result for every single input pulse with a latency (input-output delay) lower than 30 ns, including the response of the SPADs, which also allows its application as a communication receiver, quantum discrimination device, or for a feedback operation. The use of independent detectors and well-balanced coincidence circuitry completely removes any cross talk between the histogram channels, see Fig. 2(a). The effects of dark counts and afterpulses are virtually eliminated by operating the detector in the pulse regime with the repetition rate below 5 MHz. The period between individual measurement runs can be ultimately decreased to be only slightly longer than the recovery time of the constituent single-photon detectors, provided that afterpulsing is low enough. Furthermore, differences in SPAD efficiencies and other optical imperfections or imbalances of the PNRD can be arbitrarily compensated by adjusting the splitting ratios of the optical network. The result is a balanced multiplex with an overall efficiency η. This means that all systematic errors are eliminated either by design or by a sufficiently precise adjustment, independent of constituent detectors employed.

For a balanced M-channel PNRD with efficiency η, the probability of m channels clicking upon the arrival of n photons is

$$C_{mn} = \binom{M}{m} \sum_{j=0}^{m} (-1)^j \binom{m}{j} \left((1-\eta) + \frac{(m-j)\eta}{M} \right)^n. \tag{1}$$

The click statistics c_m is then determined by the photon statistics p_n [19,20,23],

$$c_m = \sum_n C_{mn} p_n. \tag{2}$$

Finding the photon statistics p_n, $n = 0, \ldots, \infty$, that satisfies the system of equations (2) for a measured click statistics c_m, $m = 0, \ldots, M$, represents the core problem of photon-statistics retrieval. This generally ill-posed problem suffers from underdetermination and sampling error. Fortunately, we have additional constraints facilitating the retrieval; i.e., the photon-number probabilities are non-negative, normalized, and typically non-negligible only within a finite range.

Here we present a novel approach, termed the expectation-maximization-entropy (EME) method, based on an expectation-maximization iterative algorithm weakly regularized by a maximum-entropy principle. The initial zeroth iteration is uniform; $p_n^{(0)} = 1/(n_{\max} + 1)$ for sufficiently large $n_{\max} \gg \langle n \rangle$. Each subsequent iteration is

$$p_n^{(k+1)} = \Pi_n^{(k)} p_n^{(k)} - \lambda (\ln p_n^{(k)} - S^{(k)}) p_n^{(k)}, \tag{3}$$

$$\Pi_n^{(k)} = \sum_{m=0}^{M} \frac{c_m}{(\sum_j C_{mj} p_j^{(k)})} C_{mn}, \qquad S^{(k)} = \sum_{n=0}^{n_{\max}} p_n^{(k)} \ln p_n^{(k)}. \tag{4}$$

Here the superscript (k) denotes the k th iteration. Each iteration is evaluated for $n = 1, \ldots, n_{\max}$. The $\Pi_n^{(k)}$ is a function of the measured click statistics c_m and the efficiency η determined by a separate measurement. $S^{(k)}$ is a negative von Neumann entropy. The parameter λ scales the entropy regularization relative to the likelihood maximization; we use a fixed value of 10^{-3} for all the photon statistics. The process is stopped when two subsequent iterations are practically identical. The retrieved statistics does not change for different initial iterations. The derivation of the algorithm is given in the Supplemental Material [36].

To show the accuracy and the robustness of the novel EME method, a numerical analysis was performed for 25 various photon statistics with different mean photon numbers. We compared the EME method with other frequently used algorithms—direct inversion and the expectation-maximization (EM) method based on likelihood maximization. EME was found to be a unique estimator that guarantees non-negativity and the absence of numerical artifacts in the retrieved photon statistics. Total variation distance $\Delta = \sum_n |p_n - p_n^{\text{true}}|/2$ between the retrieved distribution and the true one is on the order of $\sim 10^{-3}$, one order of magnitude smaller than in the case of direct inversion and maximum-likelihood approaches. Numerical simulations yield average fidelity values $\bar{F} = 0.9996$ using the EME algorithm and $\bar{F} = 0.997$ using the maximum-likelihood approach. The fidelity, defined as $F = (\sum_{n=0}^{n_{\max}} \sqrt{p_n p_n^{\text{true}}})^2$, cannot be evaluated for direct inversion due to negative values of estimated photon statistics.

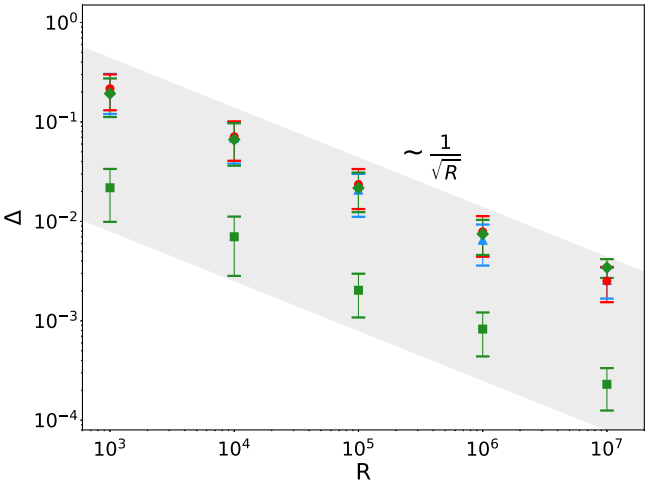

FIG. 3. A numerical analysis of EME total variation distance Δ. With more measurement runs R, the statistical error in the data is lower and the EME result approaches the true photon statistics despite the limited number of channels $M = 10$. Here shown are coherent state with $\langle n \rangle = 10$ (blue triangle up), thermal state with $\langle n \rangle = 5$ (red circle), N_p-photon cluster with $N_p = 1$ (green square), and $N_p = 9$ (green rhombus) for a single value of $\lambda = 10^{-3}$. The gray area illustrates the observed scaling $(0.25/\sqrt{R}–14/\sqrt{R}.)$

In Fig. 3, we show by numerical simulation that the results of the EME algorithm approach the respective theoretical expectations as more data are acquired. This means that, despite a limited number of channels $M = 10$, the chief source of error is the sampling error. We also verified that Δ stays the same if both the mean number of photons and the number of channels are doubled. Therefore, EME scales well to high photon numbers considering limited experimental resources. The precision of the photon-statistics retrieval can be further increased by optimizing over multiple parameters, such as M, λ, $n_{\max}$, or iteration cutoff. Eventually, Δ becomes limited by machine precision and computation time. The analysis of the complex interaction of these parameters will be the subject of further research. We also found that the EME convergence is 10–1000× faster than the plain EM approach (see

TABLE I. The comparison of EM and EME results for the measured data. Coherent state $\langle n\rangle = 4.95(2)$, thermal state $\langle n\rangle = 4.93(4)$, two-photon-subtracted thermal state $\langle n\rangle = 5.77(2)$, single-photon state $N_p = 1$, and nine-photon cluster $N_p = 9$. Both fidelity F and total variation distance Δ are shown. Standard deviations are evaluated by repeating the measurement and data processing ten times. The large distances observed for EM stem from overfitting the ill-posed problem. This is discussed in the Supplemental Material [36].

	Coherent		Thermal		Two-photon-subtracted thermal		Single photon		Nine-photon cluster	
	EM	EME	EM	EME	EM	EME	EM	EME	EM	EME
F	0.6(1)	0.9984(9)	0.69(2)	0.9978(5)	0.90(1)	0.9990(4)	0.993 94(2)	0.999 12(1)	0.5467(2)	0.999 30(2)
Δ	0.50(9)	0.002(9)	0.35(1)	0.033(3)	0.21(1)	0.019(6)	0.074 24(1)	0.000 88(1)	0.1752(5)	0.004 07(1)

the Supplemental Material [36]), while yielding significantly better results.

In our experimental demonstration, we used a balanced ten-channel configuration of the detector. We analyzed coherent states, thermal states, multimode thermal states, single-photon and multiple-photon-subtracted thermal states, and nonclassical multiphoton states. Furthermore, we have varied the mean number of photons, the number of modes, and the number of subtracted or superimposed photons. For each retrieved photon statistics we computed $\langle n\rangle$, $g^{(2)}$, and other quantities presented in detail in the Supplemental Material [36].

The measurements were performed using 1-ns-long optical pulses with the repetition rate of 2 MHz. We prepared the initial coherent signal by using a gain-switched laser diode at 810 nm. The resulting coherent pulses measured by the PNRD show almost perfect Poissonian statistics with $g^{(2)} = 1$ up to $\langle n\rangle = 20$ with average fidelity $\bar{F} = 0.996$ and total variation distance $\bar{\Delta} = 24 \times 10^{-3}$. The thermal state is generated by temporal intensity modulation of the initial coherent light by a rotating ground glass. The scattered light is collected using a single-mode optical fiber. We measured almost ideal Bose-Einstein photon statistics depicted in Fig. 2(b) with $g^{(2)} = 2$ up to $\langle n\rangle = 5$, $\langle \Delta n^2\rangle = 30$ with $\bar{F} = 0.997$ and $\bar{\Delta} = 24 \times 10^{-3}$. We varied the number of the collected thermal modes, which yielded a signal governed by Mandel-Rice statistics, going from Bose-Einstein to Poisson distribution as the number of modes increased. Multiple-photon subtraction from the thermal state was implemented using a beam splitter with a 5% reflectance. When a (multi)coincidence was detected by a multichannel single-photon detector in the reflected port, the heralded optical signal in the transmitted port was analyzed by the reported PNRD. A typical result of two-photon subtraction is shown in Fig. 2(c). Increasing the number of subtracted photons results in a transition from super-Poissonian chaotic light to a Poissonian signal [90,91]. Furthermore, we generated multiphoton states by mixing incoherently several single-photon states from spontaneous parametric down-conversion using time multiplexing. N_p successive time windows, where a single photon was heralded, were merged into a single temporal detection mode. This source emulates the collective emission from identical independent single emitters [5,9,11]. The resulting photon statistics measured for these highly nonclassical multiphoton states corresponds extremely well to the ideal attenuated N_p-photon states, see Figs. 2(d) and 2(e) for $N_p = 1$ and 9 with $\bar{F} = 0.999$ and $\bar{\Delta} = 3 \times 10^{-3}$. Also the $g^{(2)}$ parameter computed from the measured photon statistics perfectly agrees with the theoretical model $1 - 1/N_p$, see Fig. 1.

We utilize fidelity and total variation distance to compare the measured distribution with the ideal one. The worst and the best fidelities $F = 0.985$ and 0.9999 are reached across all the tested sources with average fidelity being $\bar{F} = 0.998$. The average distance is $\bar{\Delta} = 17 \times 10^{-3}$ for all the tested sources. For detailed data and comparison to plain EM, see Table I and the Supplemental Material [36]. The errors of EME are caused by slight imbalances of splitting ratios in the PNRD, variations in PNRD efficiency η, and imperfections of the tested sources, which renders the actual accuracy of the PNRD even higher. Particularly, accurate preparation and characterization of thermal and superchaotic states are highly nontrivial tasks subject to ongoing research [13,92–94].

To conclude, we have reported a fully reconfigurable near-ideal photon-number-resolving detection scheme with custom electronic processing and a novel EME photon-statistics retrieval method. The PNRD design is free of systematic errors, which are either negligible or can be arbitrarily decreased by the user. We have demonstrated exceptional accuracy of detected photon statistics that goes beyond the conventional limit of the number of PNRD channels. We measured dozens of various photonic sources ranging from highly nonclassical quantum states of light to chaotic optical signals. The results were obtained from raw data with no other processing than EME and without any demanding detector characterization. Despite uncorrected systematic errors and significant variability of the input signal, our approach shows superior fidelity across the board with typical values exceeding 99.8% for mean photon numbers up to 20 and the $g^{(2)}$ parameter reaching down to a fraction of a percent. Though having been demonstrated with common single-photon avalanche diodes, the reported measurement workflow is independent of the detection technology and can accommodate any on-off

detectors. Furthermore, the multichannel scheme allows for straightforward on-chip integration. Therefore, further improvements in speed, efficiency, and compactness can be expected using superconducting single-photon detectors [26,29,31] coupled with waveguide technology [95–97].

We acknowledge the support from the Czech Science Foundation under the Project No. 17-26143S. This work has received national funding from the MEYS and the funding from European Union's Horizon 2020 research and innovation framework programme under Grant Agreement No. 731473 (project 8C18002). Project HYPER-U-P-S has received funding from the QuantERA ERA-NET Cofund in Quantum Technologies implemented within the European Union's Horizon 2020 Programme. We also acknowledge the support from Palacký University (Projects No. IGA-PrF-2018-010 and No. IGA-PrF-2019-010).

*jezek@optics.upol.cz

[1] J. L. O'Brien, A. Furusawa, and J. Vučković, Nat. Photonics **3**, 687 (2009).
[2] J. C. F. Matthews, X.-Q. Zhou, H. Cable, P. J. Shadbolt, D. J. Saunders, G. A. Durkin, G. J. Pryde, and J. L. O'Brien, npj Quantum Inf. **2**, 16023 (2016).
[3] S. Slussarenko, M. M. Weston, H. M. Chrzanowski, L. K. Shalm, V. B. Verma, S. W. Nam, and G. J. Pryde, Nat. Photonics **11**, 700 (2017).
[4] G. Harder, T. J. Bartley, A. E. Lita, S. W. Nam, T. Gerrits, and C. Silberhorn, Phys. Rev. Lett. **116**, 143601 (2016).
[5] I. Straka, L. Lachman, J. Hloušek, M. Miková, M. Ježek, and R. Filip, npj Quantum Inf. **4**, 4 (2018).
[6] J. F. Dynes, M. Lucamarini, K. A. Patel, A. W. Sharpe, M. B. Ward, Z. L. Yuan, and A. J. Shields, Opt. Express **26**, 22733 (2018).
[7] M. D. Vidrighin, O. Dahlsten, M. Barbieri, M. S. Kim, V. Vedral, and I. A. Walmsley, Phys. Rev. Lett. **116**, 050401 (2016).
[8] N. Cottet, S. Jezouin, L. Bretheau, P. Campagne-Ibarcq, Q. Ficheux, J. Anders, A. Auffèves, R. Azouit, P. Rouchon, and B. Huard, Proc. Natl. Acad. Sci. U.S.A. **114**, 7561 (2017).
[9] H. Ta, J. Keller, M. Haltmeier, S. K. Saka, J. Schmied, F. Opazo, P. Tinnefeld, A. Munk, and S. W. Hell, Nat. Commun. **6**, 7977 (2015).
[10] Y. Israel, R. Tenne, D. Oron, and Y. Silberberg, Nat. Commun. **8**, 14786 (2017).
[11] S. J. Sahl, S. W. Hell, and S. Jakobs, Nat. Rev. Mol. Cell Biol. **18**, 685 (2017).
[12] H. J. Kimble, M. Dagenais, and L. Mandel, Phys. Rev. Lett. **39**, 691 (1977).
[13] H. E. Kondakci, A. Szameit, A. F. Abouraddy, D. N. Christodoulides, and B. E. A. Saleh, Optica **3**, 477 (2016).
[14] The autocorrelation $g^{(2)}$ stems from the second-order optical coherence evaluated as a cross-correlation of intensity I at zero delay, $g^{(2)}(0) = \langle I(t)^2\rangle/\langle I(t)\rangle^2$. For the measured signals, we calculate its value from the obtained distribution of the number of photons n, $g^{(2)} = \langle n(n-1)\rangle/\langle n\rangle^2$.
[15] K. Stensson and G. Björk, Phys. Rev. A **98**, 033812 (2018).
[16] J. Sperling, W. R. Clements, A. Eckstein, M. Moore, J. J. Renema, W. S. Kolthammer, S. W. Nam, A. Lita, T. Gerrits, W. Vogel, G. S. Agarwal, and I. A. Walmsley, Phys. Rev. Lett. **118**, 163602 (2017).
[17] T. Gerrits, A. Lita, B. Calkins, and S. W. Nam, in *Quantum Science and Technology* (Springer International Publishing, New York, 2016), pp. 31–60.
[18] C. Cahall, K. L. Nicolich, N. T. Islam, G. P. Lafyatis, A. J. Miller, D. J. Gauthier, and J. Kim, Optica **4**, 1534 (2017).
[19] H. Paul, P. Törmä, T. Kiss, and I. Jex, Phys. Rev. Lett. **76**, 2464 (1996).
[20] J. Sperling, W. Vogel, and G. S. Agarwal, Phys. Rev. A **85**, 023820 (2012).
[21] K. Banaszek and I. A. Walmsley, Opt. Lett. **28**, 52 (2003).
[22] D. Achilles, C. Silberhorn, C. Śliwa, K. Banaszek, and I. A. Walmsley, Opt. Lett. **28**, 2387 (2003).
[23] M. J. Fitch, B. C. Jacobs, T. B. Pittman, and J. D. Franson, Phys. Rev. A **68**, 043814 (2003).
[24] J. Řeháček, Z. Hradil, O. Haderka, J. J. Peřina, and M. Hamar, Phys. Rev. A **67**, 061801(R) (2003).
[25] J. Tiedau, E. Meyer-Scott, T. Nitsche, S. Barkhofen, T. J. Bartley, and C. Silberhorn, Opt. Express **27**, 1 (2019).
[26] A. Divochiy, F. Marsili, D. Bitauld, A. Gaggero, R. Leoni, F. Mattioli, A. Korneev, V. Seleznev, N. Kaurova, O. Minaeva, G. Gol'tsman, K. G. Lagoudakis, M. Benkhaoul, F. Lévy, and A. Fiore, Nat. Photonics **2**, 302 (2008).
[27] A. Allevi, M. Bondani, and A. Andreoni, Opt. Lett. **35**, 1707 (2010).
[28] D. A. Kalashnikov, S. H. Tan, M. Chekhova, and L. A. Krivitsky, Opt. Express **19**, 9352 (2011).
[29] F. Mattioli, Z. Zhou, A. Gaggero, R. Gaudio, R. Leoni, and A. Fiore, Opt. Express **24**, 9067 (2016).
[30] J. Krger, T. Ahrens, J. Sperling, W. Vogel, H. Stolz, and B. Hage, J. Phys. B **50**, 214003 (2017).
[31] D. Zhu, Q.-Y. Zhao, H. Choi, T.-J. Lu, A. E. Dane, D. Englund, and K. K. Berggren, Nat. Nanotechnol. **13**, 596 (2018).
[32] B. Calkins, P. L. Mennea, A. E. Lita, B. J. Metcalf, W. S. Kolthammer, A. Lamas-Linares, J. B. Spring, P. C. Humphreys, R. P. Mirin, J. C. Gates, P. G. R. Smith, I. A. Walmsley, T. Gerrits, and S. W. Nam, Opt. Express **21**, 22657 (2013).
[33] M. Mičuda, O. Haderka, and M. Ježek, Phys. Rev. A **78**, 025804 (2008).
[34] J. S. Lundeen, A. Feito, H. Coldenstrodt-Ronge, K. L. Pregnell, Ch. Silberhorn, T. C. Ralph, J. Eisert, M. B. Plenio, and I. A. Walmsley, Nat. Phys. **5**, 27 (2009).
[35] P. Rath, O. Kahl, S. Ferrari, F. Sproll, G. Lewes-Malandrakis, D. Brink, K. Ilin, M. Siegel, C. Nebel, and W. Pernice, Light Sci. Appl. **4**, e338 (2015).
[36] See Supplemental Material at http://link.aps.org/supplemental/10.1103/PhysRevLett.123.153604 for full details about the experimental setup, the verification of its operation, and the comparison of photon-statistic retrieval methods, which includes Refs. [37–89].
[37] L. Mandel, Opt. Lett. **4**, 205 (1979).
[38] E. J. O'Reilly and A. Olaya-Castro, Nat. Commun. **5**, 3012 (2014).
[39] P. Grangier, G. Roger, and A. Aspect, Europhys. Lett. **1**, 173 (1986).

[40] L. Lachman and R. Filip, Opt. Express **24**, 27352 (2016).
[41] M. G. Genoni, M. L. Palma, T. Tufarelli, S. Olivares, M. S. Kim, and M. G. A. Paris, Phys. Rev. A **87**, 062104 (2013).
[42] J. Park, J. Zhang, J. Lee, S.-W. Ji, M. Um, D. Lv, K. Kim, and H. Nha, Phys. Rev. Lett. **114**, 190402 (2015).
[43] J. Park, Y. Lu, J. Lee, Y. Shen, K. Zhang, S. Zhang, M. S. Zubairy, K. Kim, and H. Nha, Proc. Natl. Acad. Sci. U.S.A. **114**, 891 (2017).
[44] L. Happ, M. A. Efremov, H. Nha, and W. P. Schleich, New J. Phys. **20**, 023046 (2018).
[45] I. Straka, A. Predojević, T. Huber, L. Lachman, L. Butschek, M. Miková, M. Mičuda, G. S. Solomon, G. Weihs, M. Ježek, and R. Filip, Phys. Rev. Lett. **113**, 223603 (2014).
[46] A. Mandarino, M. Bina, C. Porto, S. Cialdi, S. Olivares, and M. G. A. Paris, Phys. Rev. A **93**, 062118 (2016).
[47] M. A. Wayne, J. C. Bienfang, and S. V. Polyakov, Opt. Express **25**, 20352 (2017).
[48] A. W. Ziarkash, S. K. Joshi, M. Stipčević, and R. Ursin, Sci. Rep. **8**, 5076 (2018).
[49] M. Fujiwara, A. Tanaka, S. Takahashi, K. Yoshino, Y. Nambu, A. Tajima, S. Miki, T. Yamashita, Z. Wang, A. Tomita, and M. Sasaki, Opt. Express **19**, 19562 (2011).
[50] V. Burenkov, H. Xu, B. Qi, R. H. Hadfield, and H.-K. Lo, J. Appl. Phys. **113**, 213102 (2013).
[51] W. Martienssen and E. Spiller, Am. J. Phys. **32**, 919 (1964).
[52] I. Straka, J. Mika, and M. Ježek, Opt. Express **26**, 8998 (2018).
[53] J. Hloušek, M. Ježek, and R. Filip, Sci. Rep. **7**, 13046 (2017).
[54] Yu. I. Bogdanov, K. G. Katamadze, G. V. Avosopiants, L. V. Belinsky, N. A. Bogdanova, A. A. Kalinkin, and S. P. Kulik, Phys. Rev. A **96**, 063803 (2017).
[55] S. M. Barnett, G. Ferenczi, C. R. Gilson, and F. C. Speirits, Phys. Rev. A **98**, 013809 (2018).
[56] I. A. Fedorov, A. E. Ulanov, Y. V. Kurochkin, and A. I. Lvovsky, Optica **2**, 112 (2015).
[57] K. G. Katamadze, G. V. Avosopiants, Y. Bogdanov, and S. P. Kulik, Optica **5**, 723 (2018).
[58] L. Qi, M. Manceau, A. Cavanna, F. Gumpert, L. Carbone, M. de Vittorio, A. Bramati, E. Giacobino, L. Lachman, R. Filip, and M. Chekhova, New J. Phys. **20**, 073013 (2018).
[59] L. Lachman, I. Straka, J. Hloušek, M. Ježek, and R. Filip, Phys. Rev. Lett. **123**, 043601 (2019).
[60] A. Luis and L. L. Sánchez-Soto, Phys. Rev. Lett. **83**, 3573 (1999).
[61] J. Fiurášek, Phys. Rev. A **64**, 024102 (2001).
[62] J. Řeháček, D. Mogilevtsev, and Z. Hradil, Phys. Rev. Lett. **105**, 010402 (2010).
[63] C. M. Natarajan, L. Zhang, H. Coldenstrodt-Ronge, G. Donati, S. N. Dorenbos, V. Zwiller, I. A. Walmsley, and R. H. Hadfield, Opt. Express **21**, 893 (2013).
[64] M. Altorio, M. G. Genoni, F. Somma, and M. Barbieri, Phys. Rev. Lett. **116**, 100802 (2016).
[65] M. Cooper, M. Karpiński, and B. J. Smith, Nat. Commun. **5**, 4332 (2014).
[66] C. R. Rao and S. K. Mitra, *Generalized Inverse of Matrices and Its Applications* (Wiley, New York, 1971).
[67] A. Ben-Israel and T. N. E. Greville, *Generalized Inverses—Theory and Applications* (Springer-Verlag, Berlin, 2003).
[68] A. N. Tikhonov, Dokl. Akad. Nauk SSSR **39**, 195 (1943).
[69] A. E. Hoerl, Chem. Eng. Prog. **58**, 54 (1962).
[70] A. N. Tikhonov, A. Goncharsky, V. V. Stepanov, and A. G. Yagola, *Numerical Methods for the Solution of Ill-Posed Problems* (Springer-Verlag, Berlin, 1995).
[71] V. N. Starkov, A. A. Semenov, and H. V. Gomonay, Phys. Rev. A **80**, 013813 (2009).
[72] A. P. Dempster, N. M. Laird, and D. B. Rubin, J. R. Stat. Soc. Ser. B **39**, 1 (1977).
[73] Y. Vardi and D. Lee, J. R. Stat. Soc. Ser. B **55**, 569 (1993).
[74] K. Banaszek, Phys. Rev. A **57**, 5013 (1998).
[75] F. Marsili, D. Bitauld, A. Gaggero, S. Jahanmirinejad, R. Leoni, F. Mattioli, and A. Fiore, New J. Phys. **11**, 045022 (2009).
[76] K. Banaszek, Acta Phys. Slovaca **48**, 185 (1998).
[77] G. Zambra, A. Andreoni, M. Bondani, M. Gramegna, M. Genovese, G. Brida, A. Rossi, and M. G. A. Paris, Phys. Rev. Lett. **95**, 063602 (2005).
[78] *Maximum-Entropy and Bayesian Methods in Inverse Problems*, edited by C. R. Smith and W. T. Grandy (Springer, Netherlands, 1985).
[79] R. L. Parker, *Geophysical Inverse Theory* (Princeton University Press, Princeton, NJ, 1994).
[80] Y. Grandvalet and Y. Bengio, in *Advances in Neural Information Processing Systems 17*, edited by L. K. Saul, Y. Weiss, and L. Bottou (MIT Press, Cambridge, MA, 2005), pp. 529–536.
[81] Y. S. Teo, H. Zhu, B.-G. Englert, J. Řeháček, and Z. Hradil, Phys. Rev. Lett. **107**, 020404 (2011).
[82] A. I. Lvovsky and M. G. Raymer, Rev. Mod. Phys. **81**, 299 (2009).
[83] M. A. Golub, Opt. Photonics News **15**, 36 (2004).
[84] A. Hermerschmidt, S. Krüger, and G. Wernicke, Opt. Lett. **32**, 448 (2007).
[85] M. M. Rajadhyaksha and R. H. Webb, Appl. Opt. **34**, 8066 (1995).
[86] J. C. F. Matthews, A. Politi, A. Stefanov, and J. L. O'Brien, Nat. Photonics **3**, 346 (2009).
[87] B. J. Smith, D. Kundys, N. Thomas-Peter, P. G. R. Smith, and I. A. Walmsley, Opt. Express **17**, 13516 (2009).
[88] F. Flamini, L. Magrini, A. S. Rab, N. Spagnolo, V. D'Ambrosio, P. Mataloni, F. Sciarrino, T. Zandrini, A. Crespi, R. Ramponi, and R. Osellame, Light Sci. Appl. **4**, e354 (2015).
[89] J. Carolan, C. Harrold, C. Sparrow, E. Martin-Lopez, N. J. Russell, J. W. Silverstone, P. J. Shadbolt, N. Matsuda, M. Oguma, M. Itoh, G. D. Marshall, M. G. Thompson, J. C. F. Matthews, T. Hashimoto, J. L. O'Brien, and A. Laing, Science **349**, 711 (2015).
[90] A. Allevi, A. Andreoni, M. Bondani, M. G. Genoni, and S. Olivares, Phys. Rev. A **82**, 013816 (2010).
[91] Y. Zhai, F. E. Becerra, B. L. Glebov, J. Wen, A. E. Lita, B. Calkins, T. Gerrits, J. Fan, S. W. Nam, and A. Migdall, Opt. Lett. **38**, 2171 (2013).
[92] A. Allevi and M. Bondani, Opt. Lett. **40**, 3089 (2015).
[93] J. Mika, L. Podhora, L. Lachman, P. Obšil, J. Hloušek, M. Ježek, R. Filip, and L. Slodička, New J. Phys. **20**, 093002 (2018).

[94] M. Manceau, K. Y. Spasibko, G. Leuchs, R. Filip, and M. Chekhova, Phys. Rev. Lett. **123**, 123606 (2019).
[95] D. Sahin, A. Gaggero, Z. Zhou, S. Jahanmirinejad, F. Mattioli, R. Leoni, J. Beetz, M. Lermer, M. Kamp, S. Höfling, and A. Fiore, Appl. Phys. Lett. **103**, 111116 (2013).
[96] R. Heilmann, J. Sperling, A. Perez-Leija, M. Gräfe, M. Heinrich, S. Nolte, W. Vogel, and A. Szameit, Sci. Rep. **6**, 19489 (2016).
[97] J. Münzberg, A. Vetter, F. Beutel, W. Hartmann, S. Ferrari, W. H. P. Pernice, and C. Rockstuhl, Optica **5**, 658 (2018).